REVISTA MEXICANA DE FÍSICA S **52** (4) 17–22 NOVIEMBRE 2006

Nuclear mass prediction as an image reconstruction problem: can observed pattern determine mass values?

A. Frank, J.C. López Vieyra, I. Morales Agiss, J. Barea, and J.G. Hirsch
Instituto de Ciencias Nucleares, Universidad Nacional Autónoma de México, Apartado Postal 70-543, 04510 México, D.F.

V. Velázquez
Facultad de Ciencias, Universidad Nacional Autónoma de México, 04510 México, D.F.

P. Van Isacker
GANIL, BP 55027, F-14076 Caen Cedex 5, France.

Recibido el 8 de marzo de 2006; aceptado el 9 de abril de 2006

Theoretical prediction of nuclear masses is analyzed as a pattern recognition problem on the N-Z plane. A global pattern is observed by plotting the differences between measured masses and Liquid Drop Model (LDM) predictions. After unfolding the data by removing the smooth LDM mass contributions, the remaining microscopic effects have proved difficult to model, although they display a striking pattern. These deviations carry information related to shell closures, nuclear deformation and the residual nuclear interactions. In the present work the more than 2000 known nuclear masses are studied as an array in the N-Z plane viewed through a mask, behind which the approximately 7000 unknown unstable nuclei that can exist between the proton and neutron drip lines are hidden. We show here that employing a Fourier transform deconvolution method these by masses can be predicted with similar accuracy than standard methods. We believe that a more general approach needs to be implemented, however, to optimize the procedures predictive power. Thus, while we see the need to study and implement alternative image reconstruction and extrapolation methods, the general ideas are already contained in this paper.

Keywords: Nuclear masses; image reconstruction; Fourier transform; deconvolution.

La predicción teórica de masas nucleares es analizada como un problema de reconocimiento de patrones en el plano N-Z. Al graficar las diferencias entre las masas medidas y las predicciones del modelo de la gota (LDM) se obtiene un claro patrón. La predicción de los efectos microscópicos evidentes en este patrón ha mostrado ser una ardua tarea. Las desviaciones de las masas nucleares respecto de la gota contienen información asociada a capas cerradas, a deformaciones y a los efectos de la interacción nuclear residual. En este trabajo se estudian las más de 2000 masas nucleares conocidas como un arreglo en el plano N-Z, visto a través de una máscara detrás de la cual se ocultan las cerca de 7000 masas de núcleos inestables, desconocidas actualmente, que pueden existir entre las líneas de estabilidad de emisión de un protón o de un neutrón. Empleando el método de deconvolución de las tranformadas de Fourier, las masas conocidas pueden ser reproducidas con una precisón similar a la lograda con los métodos tradicionales. Sin embargo, se requiere un procedimiento más general para optimizar el poder predictivo del método. Si bien las ideas básicas están contenidas en el presente trabajo, es necesario investigar e implementar métodos altenativos de reconstrucción y de extrapolación de imágenes.

Descriptores: Masas nucleares; recontrucción de imáges; transformada de Fourier; deconvolución.

PACS: 32.10.Bi; 07.05.Pj; 02.30.Nw

1. Introduction

An accurate knowledge of nuclear masses is required to understand fundamental processes in nuclear physics [1]. Though much progress has been made in measuring the masses of exotic nuclei, theoretical models are necessary to *predict* them in regions far from stability [2]. Nuclear mass prediction has become a crucial ingredient for the calculations required in nuclear astrophysics. The simplest example is that of the liquid drop model (LDM), which incorporates the essential macroscopic terms, the nucleus being pictured as a very dense, charged liquid drop, and including other important nuclear effects, such as the pairing interactions. The finite range droplet model (FRDM) [3], which combines the macroscopic effects with microscopic shell and pairing corrections, has become the *de facto* standard for mass formulas. A microscopically inspired model has been introduced by Duflo and Zuker (DZ) [4] with surprisingly good results. Finally, among other mean-field methods it is worth mentioning the Skyrme-Hartree-Fock approach [5],which leads to mass formulas that calculate the masses (and often other properties) of as many as 8979 nuclides, although its predictability has not been too impressive. More troublesome is the fact that different approaches tend to diverge from each other in their predictions, so there is a permanent search for better theoretical models that reduce the difference with the experimental masses and produce reliable predictions for unstable nuclei.

Besides the "global" formulas of which the FRDM method has become the standard, there are a number of "'local" mass formulas. These local methods are usually effective when calculating the mass of a nucleus, or a set of nuclei, which are fairly close to nuclei of known mass, taking

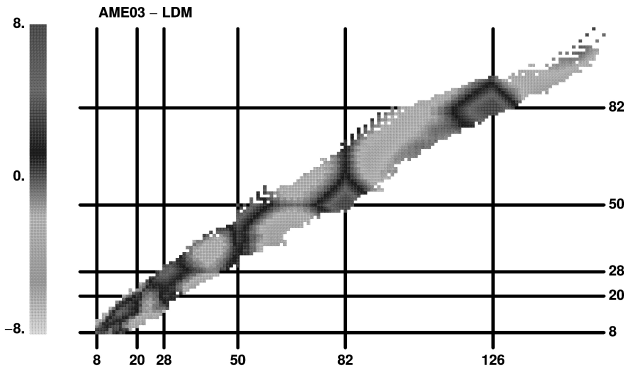

FIGURE 1. Nuclear mass differences in the nuclear landscape. The horizontal axis corresponds to *neutron number* N. The vertical axis corresponds to *atomic number* Z.

advantage of the relative smoothness of the masses M(Z,N) as a function of proton (Z) and neutron (N) numbers to deduce systematic trends. Among these methods, there are a set of algebraic relations for nuclear neighbors known as the Garvey-Kelson (GK) relations, which can be deduced from an extreme single-particle picture of nuclei [6].

Detailed analyses of nuclear mass errors have been performed, using the FRDM [3], the shell-model-inspired mass calculations of Duflo and Zuker (DZ) [4], the Hartree-Fock-Bogoliubov mass calculations of Goriely et al. [5], as well as other methods, including the Garvey-Kelson (GK) relations [6]. The presence of strong correlations between mass errors calculated in a mean-field approach in neighboring nuclei has been exhibited, as well as the existence of a well defined chaotic signal in its power spectrum, but further analysis demonstrates that the inclusion of many-body interactions or the introduction of local information removes the chaotic signal [7, 8].

In this paper a new approach to the problem of nuclear predictions is introduced. The starting point is the striking color-coded pattern observed on the nuclear landscape when taking the differences between Liquid Drop Model (LDM) predictions [9] and measured masses [10], as shown in Fig. 1.

After removing the smooth LDM mass contributions, what remains are the microscopic components, which have proved difficult to predict by the different methods, all of which attempt to minimize the differences with measured masses. The residual pattern observed in Fig. 1, however, is quite remarkable and suggests a different approach. These residual "unfolded" data contain information related with shell closures, nuclear deformations, and the residual nuclear interaction, in a compelling graphic form. We therefore suggest that the approximately 2000 known nuclear masses can be studied as an array in the N-Z plane viewed through a window. The remaining nuclei (approximately 7000 of them) which can exist between the proton and neutron drip lines, lie hidden, covered by a "mask". So the question is how to "open the window" and watch and scrutinize the rest of the pattern. We show here that by employing a Fourier transform deconvolution method these masses can be predicted with similar accuracy than standard methods. Other approaches need to be studied and implemented (one of which we briefly discuss below) to optimize the procedures predictive power [11]. In the following sections the deconvolution approach is briefly described and some preliminary results presented.

2. Mathematical Formulation of the problem

The first step in our analysis consists in translating the nuclear mass table into an image. A standard two dimensional array is built in which the horizontal position corresponds to the number of neutrons and the vertical position to the number of protons. Differences between experimental mass values and those calculated using the liquid drop model for each isotope define the function

$$i(n,z) = m^{exp}(n,z) - m^{LDM}(n,z), \tag{1}$$

which is plotted in the (n,z) plane introducing a color code associated with the mass deviations, as shown in Fig. 1. As both the proton and neutron numbers are integers, this is a discrete function defined in a restricted domain of $\mathbb{I}^2$. It is appropriate to emphasize that $i(n,z)$ is only defined in the limited region where measured masses $m^{exp}(n,z)$ are known, *i.e.* the colored region in Fig. 1. It can be extended to the whole N-Z rectangle of interest by assigning null values to addresses where there are no measured experimental masses.

To predict the nuclear mass differences $m(n,z)$ along the whole rectangle, a binary mask function $w(n,z)$ is introduced. This mask takes the value 1 for those positions n and z on which the experimental nuclear masses are known, and 0 on the others. This procedure, however, can be made more general by assigning a different value to $w(n,z)$ in the region where the masses are known, in order to emphasize the importance of, for example, the boundary region in Fig. 1. In this way the extrapolation can be made more reliable [11]. In this paper we shall henceforth confine our analysis to a binary mask. Known mass differences $i(n,z)$ are related to the total mass differences $m(n,z)$ by

$$i(n,z) = m(n,z) \cdot w(n,z). \tag{2}$$

In order to predict unknown masses, we need to extract $m(n,z)$ from Eq. (2). Formally, this is a deconvolution problem, which can be solved using discrete Fourier transforms. If $I(k_n,k_z)$, $M(k_n,k_z)$ and $W(k_n,k_z)$ are the Fourier transforms of $i(n,z)$, $m(n,z)$ and $w(n,z)$, respectively, the Fourier transform of Eq. (2) is given by

$$I(k_n,k_z) = (M * W)(k_n,k_z), \tag{3}$$

where $(M*W)$ represents the convolution of the functions M and W. Given that both $i(n,z)$ and $w(n,z)$ are known for the whole rectangular domain, their Fourier transforms $I(k_n,k_z)$ and $W(k_n,k_z)$ can be evaluated directly. The problem is narrowed to obtaining the function $M(k_n,k_z)$ (the discrete Fourier transform of $m(n,z)$), from which $m(n,z)$ can be recovered applying the inverse Fourier transform.

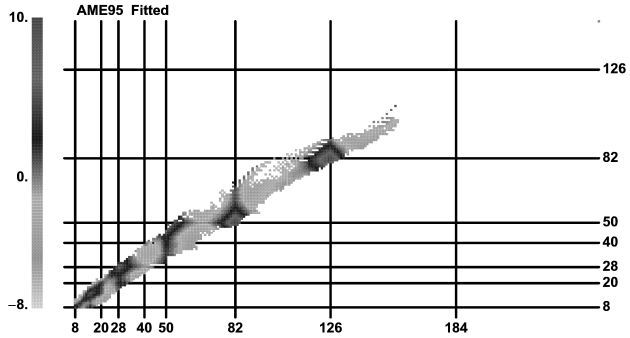

FIGURE 2. Reconstructed image of the nuclear mass differences "AME95 vs ILDM" after 200 iterations.

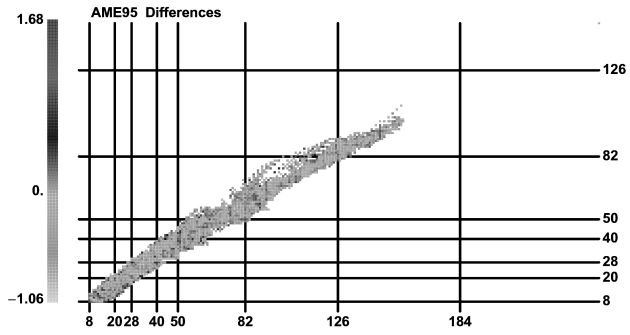

FIGURE 3. Differences Experimental vs Reconstructed "AME95 vs ILDM" after 200 iterations.

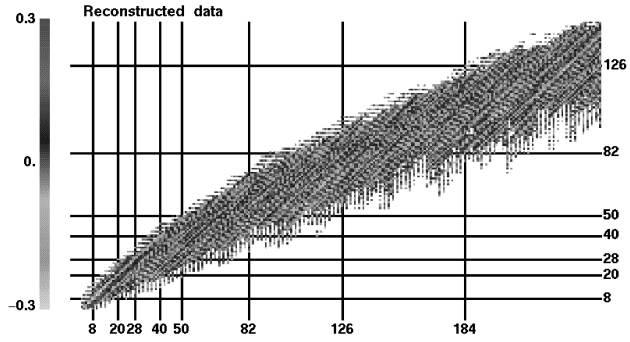

FIGURE 4. Garvey-Kelson deviations map calculated using the GK relations iteratively.

Deconvolution is usually non-trivial and may lead to non-unique solutions, but there exist several linear algorithms, such as the inverse filtering and the Wiener filtering, and non-linear algorithms, such as the CLEAN method, the maximum entropy method (MEM) and LUCY, which provide testable methodologies.

The CLEAN method is a deconvolution algorithm often used in radioastronomy. We have applied a specially adapted version of the "CLEAN" algorithm, developed by Clark *et al.* [12], to the mass reconstruction problem. Our version employs a deconvolution algorithm to remove the artifacts introduced by the shape of the window (or mask), thereby allowing the Fourier analysis of non-rectangular texture patches. We assume that the "full" mass pattern $m(x, y)$ can be modeled by a finite number of harmonic components. The deconvolution algorithm proceeds by detecting which components, when corrupted by the shape mask, provide the best explanation of the patterns observed in the Fourier spectra. Each component is then relocated to the *clean spectrum* and its footprint erased from the corrupted spectrum. The process is repeated until only noise residuals are left in the corrupted spectrum. The reconstruction process is repeated for a series of boxes with different size. The reported results are obtained averaging over all boxes. Details will be published elsewhere [13].

As mentioned earlier,a more general prescription is to use a non-binary mask, that is, to assign unequal weights to different areas of the observed image, *e.g.*, ascribing in this way more importance to neighboring nuclei in the extrapolation, given the smoothness of the observed "image", Fig. 1. Further support for this idea arises from the close agreement of the nuclear mass data to the Garvey-Kelson relations [6].

3. Nuclear Forecasting as image reconstruction

The CLEAN algorithm described above was programmed in *Mathematica* and Fortran, and applied to the pattern of differences between experimental nuclear masses (AME95) [14] and the theoretically calculated masses using the Liquid Drop Model [9]. As one possible test of predictability, we compare the calculated masses using the pattern reconstruction algorithm with the data for a larger set of nuclear masses (AME03) [10]. A (consistent) calculation for the nucleon *driplines* is also included. The results are shown below.

3.1. Reconstruction of measured masses

To test the ability of the present method to reconstruct known masses, the set of 1888 nuclei whose masses were reported in AME95 [14], corrected with the AME03 [10] information, was employed as input data. Here we used $Z_{max} = 150$, $N_{max} = 250$, which allows for the exploration of possible stability islands associated with superheavy elements.

The algorithm was applied to reconstruct the "AME03 vs ILDM" data. The differences between the reconstructed masses and those obtained using the Liquid Drop Model are presented in Fig. 2. There is a clear resemblance in the plots, as seen in Fig. 1.

In order to gauge the quality of the mass reconstruction, the *rms* average error between reconstructed and experimental masses was studied. After 200 iterations (the introduction of 200 frequencies) it attains the value 0.2165 MeV, a number that can be lowered by increasing the number of steps. The differences between the experimental and reconstructed masses are plotted in Fig. 3, where we cannot detect any remaining pattern.

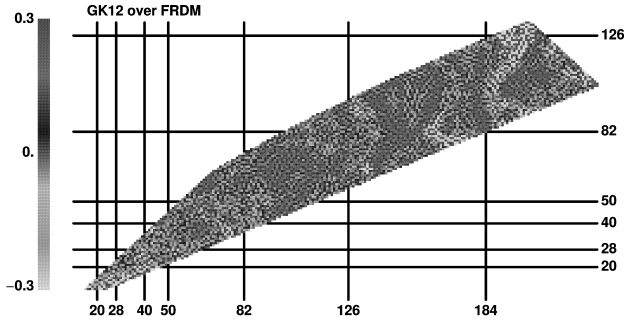

FIGURE 5. Same as Fig. 4, but using Moller and Nix mass table.

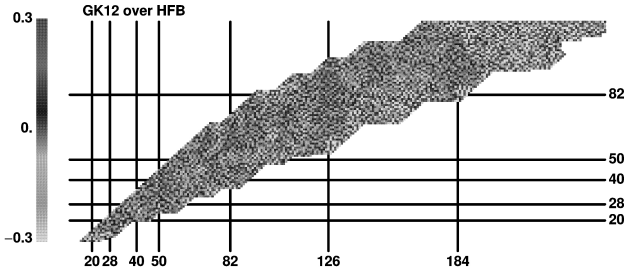

FIGURE 6. Same as Fig. 4, but using Hartree-Fock-Bogoliubov mass table.

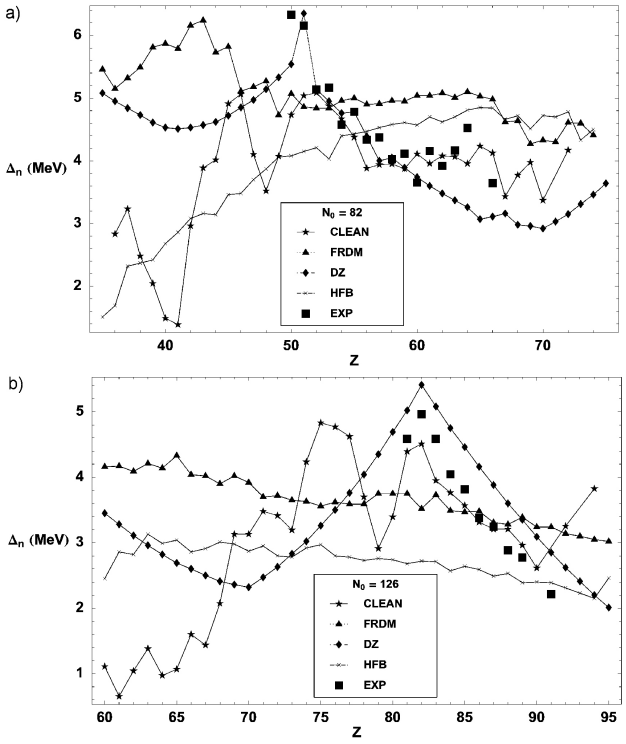

FIGURE 7. Neutron shell gaps as a function of Z for the four mass tables CLEAN, Moller and Nix (FRDM), Duflo-Zuker (DZ) and Hartree-Fock Bogoliubov (HFB).

3.2. Prediction of new masses

Besides reproducing known masses, the method predicts the masses of all possible isotopes in the area between the proton and neutron driplines. Using the reconstructed pattern the value of 289 new nuclear masses (AME03) [10] is predicted.

The new masses have an rms value of 0.800 MeV, which compares well with most mass prediction formalisms [2]. By using the masses of AME95 that were corrected in the new compilation [10], the predicted masses deviate by 0.650 MeV, a very significant improvement and a striking proof of consistency of the image reconstruction method.

A strong test which can be applied to predicted nuclear masses is provided by the Garvey-Kelson (GK) relations [6]. They are the two sets of equations connecting the masses of particular neighboring nuclei. These relations do not involve free parameters and can be derived from a simple nuclear-model picture. Strictly speaking, they do not yield an independent calculational tool, but they do provide strong indications that a large fraction of the mass values have a smooth and regular behavior. In this interpretation, the GK relations can be viewed as a simple methodology to estimate nuclear masses from those of its neighbors or, equivalently, to apply an indenpendent test of the quality of a given set of mass predictions.

It is remarkable that the GK relations are almost exactly satisfied in the predicted areas, as shown in Fig. 4, which is not the case for the FDRM and HFB calculations, as shown in Fig. 5 and 6. The DZ and LDM formulas do satisfy these relations accurately, but this is due to the simple form used for the expansion functions in N and Z [6, 13].

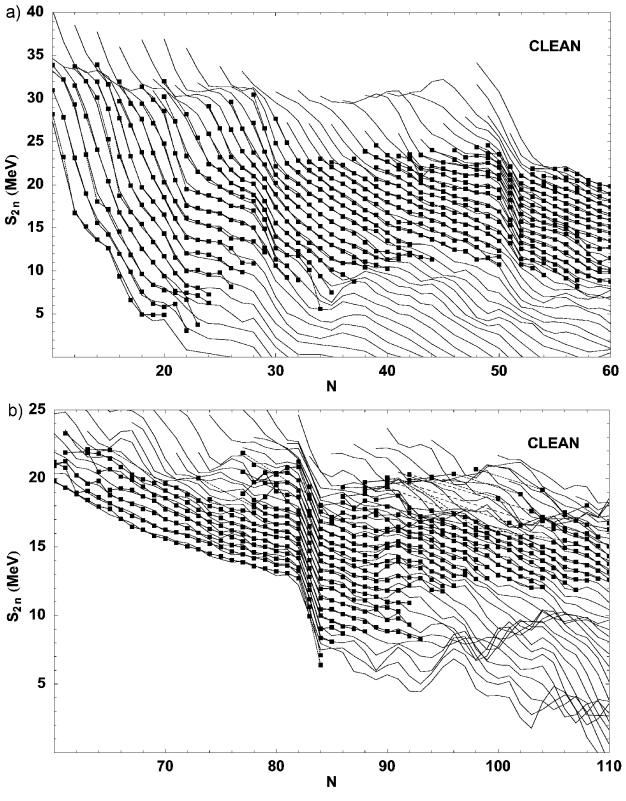

FIGURE 8. Two neutron separation energies for different isotopic chains as a function of N for the mass table CLEAN. Calculated data are indicated by continuous lines. Experimental data is marked with squares joined by dashed lines.

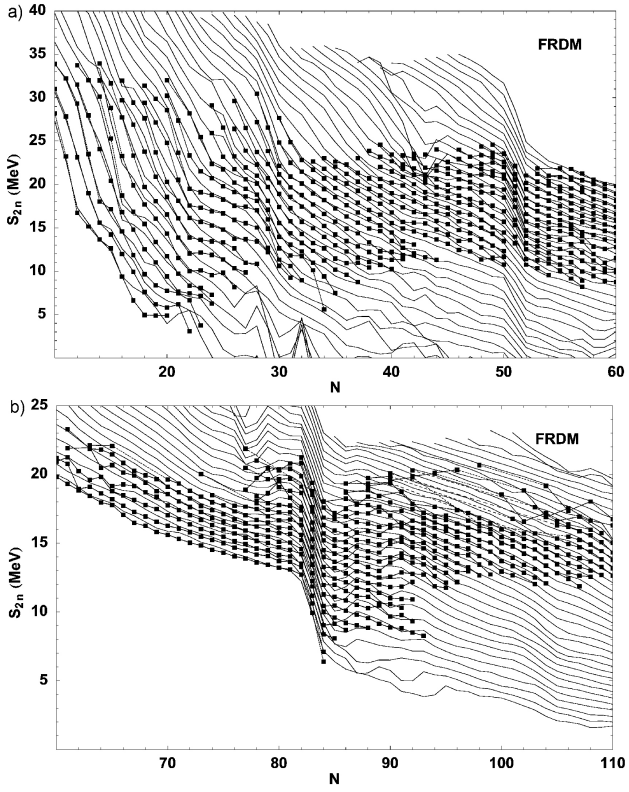

FIGURE 9. Same as Fig. 8, but using the mass table of Moller and Nix.

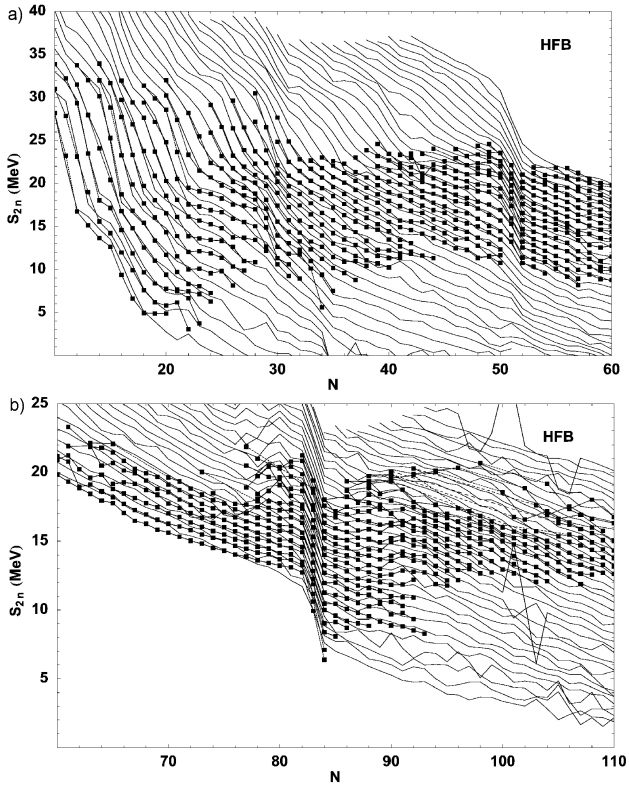

FIGURE 10. Same as Fig. 8, but using the mass table of Hartree-Fock-Bogoliubov calculations.

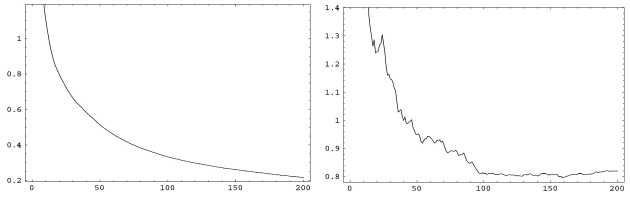

FIGURE 11. (a) RMS (input data vs reconstructed data), (b) RMS (predicted vs new AME'03 data) as a function of number of iterations. Maximum number of iterations was 200, with constant gain g=1. The rectangular grid used was $(Z_{max}, N_{max}) = (150, 250)$.

In Fig. 7 we show a comparison of the N=82 and N=126 shell gaps for different proton numbers, as given by the different models discussed in this paper. Two neutron separation energies for different isotopic chains as a function of N for the reconstructed masses are presented in Fig. 8. Calculated data are indicated by continuous lines. Experimental data is marked with squares joined by dashed lines. Shell closures at N = 28, 50 and 82 are clearly distinguished. However, these shell closures are predicted to disappear for nuclei far from stability. Two proton separation energies are plotted for the same regions as predicted by Moller and Nix in Fig 9, and by HFB calculations in Fig. 10. In both calculations the shell gaps are predicted to subsist even for extremely unstable nuclei.

3.2.1. Improving mass reconstruction

The process of mass reconstruction is performed selecting the frequency with the largest squared Fourier amplitude, filtering it through the mask and reproducing the data with it. In the following step the frequency with the second largest squared Fourier amplitude is employed, next the third, etc. The process goes on until the required precision in the data reconstruction is obtained.

In Fig. 11a the rms value of the adjusted data is shown as a function of the iteration number, *i.e.* as the number of frequencies employed in the reconstruction.

The *rms* value of fitted vs experimental data displays a monotonous decreasing behavior as the number of iterations increase. Eventually, the rms value can be reduced to very small values for a large number of iterations. The rms error after 200 iterations was 0.2165 MeV. On the other hand, the *rms* value of predicted vs experimental AME03 data displays a decreasing but non-monotonous behavior as function of the number of iterations. However, it seems that the *rms* value (predicted vs experimental AME03 data) reaches a minimal value (rms$\simeq$ 0.795 MeV) for certain number of iterations ($\sim$ 159) after which the prediction is essentially constant. The final rms after 200 iterations was 0.820 MeV. As explained before, by using the masses of AME95 that were corrected in the new compilation [10], the predicted masses deviate by only 0.650 MeV, a compelling proof of consistency of the image reconstruction method.

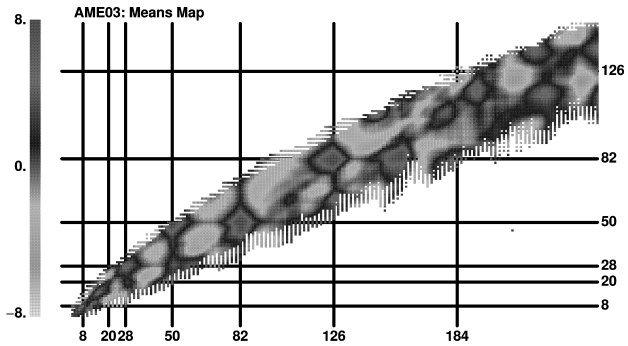

FIGURE 12. Reconstructed pattern bounded by driplines in the prediction after 200 iterations.

3.2.2. Opening the window

The reconstructed pattern allows us to enlarge the window and find the predictions all the way up to the *driplines*. The results of the 200 frequencies iteration procedure is shown in Fig. 12.

A stability island is predicted around the superheavy element $(n, z) \simeq (194, 116)$. Further work is needed to confirm the robustness of this prediction.

4. Conclusions

Pattern recognition techniques have been applied to the mass deviations obtained from the LDM formula smooth contributions. Measured masses can be reconstructed with a precision of 200 keV,while new masses from AME03 are predicted with an average error of 800 keV, diminishing to 650 keV when using the corrected AME03 masses. A new stability island is predicted around $(n, z) \simeq (194, 116)$. Other observables besides nuclear masses, like nuclear deformation and beta decay properties, may be analyzed with the same techniques.This procedure, however, can be made more general by assigning a different value to the window $w(n, z)$ in the region where the masses are known, in order to emphasize the importance of, for example, the boundary region in Fig. 1. In this way the extrapolation can be made more reliable [11]. We are currently implementing this generalization and carrying out diverse tests to study further constraints, which may include a "'maximal entropy condition"' or mathematical conditions (such as smoothness-continuity requirements) in the pattern recognition analysis, in order to achieve a more accurate and robust predictability [13].

Acknowledgments

Fruitful conversations with Ani Aprahamian, Jorge Dukelsky and Alejandro Raga are gratefully acknowledged. This work was supported in part by PAPIIT-UNAM and Conacyt-Mexico.

1. C.E. Rolfs and W.S. Rodney, *Cauldrons in the Cosmos* (University of Chicago Press, 1988).
2. D. Lunney, J.M. Pearson, and C. Thibault, *Rev. Mod. Phys.* **75** (2003) 1021.
3. P. Möller, J.R. Nix, W.D. Myers, and W.J. Swiatecki, *At. Data Nucl. Data Tables* **59** (1995) 185.
4. J. Duflo, *Nucl. Phys. A* **576** (1994 29); J. Duflo and A.P. Zuker, *Phys. Rev. C* **52** (1995) R23.
5. S. Goriely, F. Tondeur, and J.M. Pearson, *Atom. Data Nucl. Data Tables* **77** (2001) 311; M.V. Stoitsov, J. Dobaczewski, W. Nazarewicz, S. Pittel, and D.J. Dean, *Phys. Rev. C* **68** (2003) 054312.
6. G.T. Garvey and I. Kelson, *Phys. Rev. Lett.* **16** (1966) 197; G.T. Garvey, W.J. Gerace, R.L. Jaffe, I. Talmi, and I. Kelson, *Rev. Mod. Phys.* **41** (1969) S1.
7. J.G. Hirsch, V. Velázquez, and A. Frank, *Phys. Lett. B* **595** (2004) 231.
8. J. Barea, A. Frank, J.G. Hirsch, and P. van Isacker, *Phys. Rev. Lett.* **94** (2005) 102501.
9. S.R. Souza *et al.*, *Phys. Rev. C* **67** (2003) 051602(R).
10. G. Audi, A.H. Wapstra, and C. Thibault, *Nucl. Phys. A* **729** (2003) 337.
11. A. Kaup, K. Meisinger, and T. Aach, *Int. J. Electron. Commun. (AEU)* **59** (2005) 147.
12. A.A. Clark, B.T. Thomas, N.W. Campbell, and P. Greenway *"Texture Deconvolution for the Fourier-Based Analysis of Non-Rectangular Regions"*, in *British Machine Vision Conference*, pp 193–202, British Machine Vision Association, 1999.
13. J. Barea *et al.*, to be published.
14. G. Audi and A.H. Wapstra, *Nucl. Phys. A* **595** (1995) 409.